Density-Based Diamagnetic Separation: Devices for Detecting Binding Events and for Collecting Unlabeled Diamagnetic Particles in Paramagnetic Solutions

Adam Winkleman,[†] Raquel Perez-Castillejos,[†] Katherine L. Gudiksen,[†] Scott T. Phillips,[†] Mara Prentiss,[‡] and George M. Whitesides*,[†]

Department of Chemistry and Chemical Biology and Department of Physics, Harvard University, 12 Oxford Street, Cambridge, Massachusetts 02138

This paper describes the fabrication of a fluidic device for detecting and separating diamagnetic materials that differ in density. The basis for the separation is the balance of the magnetic and gravitational forces on diamagnetic materials suspended in a paramagnetic medium. The paper demonstrates two applications of separations involving particles suspended in static fluids for detecting the following: (i) the binding of streptavidin to solid-supported biotin and (ii) the binding of citrate-capped gold nanoparticles to amine-modified polystyrene spheres. The paper also demonstrates a microfluidic device in which polystyrene particles that differ in their content of CH_2Cl groups are continuously separated and collected in a flowing stream of an aqueous solution of $GdCl_3$. The procedures for separation and detection described in this paper require only gadolinium salts, two NdFeB magnets, and simple microfluidic devices fabricated from poly-(dimethylsiloxane). This device requires no power, has no moving parts, and may be suitable for use in resource-poor environments.

This paper describes the fabrication and utility of a microfluidic device for detecting and separating diamagnetic materials that differ in density. The basis for the separation is the balance of the magnetic and gravitational forces on diamagnetic materials suspended in a paramagnetic medium. We demonstrate the value of this device by (i) detecting the binding of streptavidin to polymer-supported biotin, (ii) detecting the binding of citrate-capped gold nanoparticles to amine-modified polystyrene spheres, and (iii) separating polystyrene particles that differ in CH_2Cl content within a flowing microfluidic system. The protocols for detection and separation require only gadolinium chloride (or diethylenetriaminepentaacetic acid gadolinium(III) dihydrogen salt ($Gd^{3+}\cdot DTPA$)), two NdFeB magnets, and simple microfluidic devices fabricated from poly(dimethylsiloxane) (PDMS). The simplicity and versatility of these methods make them useful for general laboratory protocols; we believe they are also suitable for use in remote locations where electricity is not available and where

portability and operational ease are essential.[1,2] We believe that these density-based detection and separation methods have the potential to be widely useful as analytical tools for the physical and biological sciences.

Magnetic labels facilitate the separation and purification of chemical and biological samples.[3,4] These labels are often superparamagnetic nano- or microspheres (e.g., Invitrogen's Dynabeads),[5] which can be covalently attached to most chemical and biological samples. For example, immunomagnetic separation employs antibodies—often monoclonal—bound to magnetic particles for the removal of prokaryotic and eukaryotic cells from suspension.[4,6] Many techniques—including cell separation,[7,8] free flow magnetophoresis,[9] and immunoassays[10]—have been developed for use in microfluidic devices for lab-on-a-chip technology.[11,12] These magnetic labeling techniques have several limitations: (i) the separations are binary; i.e., magnetic particles are separated from diamagnetic particles; (ii) the labeling of a diamagnetic material requires a chemical reaction; (iii) the presence of a magnetic particle attached to a diamagnetic material—specifically a cell, antibody, or protein—alters the functionality and properties of the surface of the material; and (iv) the magnetic label must be removed after separation to obtain a pure diamagnetic sample.

New label-free techniques for manipulating and separating diamagnetic materials in suspension that overcome these limitations would be useful. Magnetic separations are used extensively

---

(1) Yager, P.; Edwards, T.; Fu, E.; Helton, K.; Nelson, K.; Tam, M. R.; Weigl, B. H. *Nature* **2006**, *442*, 412−418.

(2) Sia, S. K.; Linder, V.; Parviz, B. A.; Siegel, A.; Whitesides, G. M. *Angew. Chem., Int. Edit.* **2004**, *43*, 498−502.

(3) Ito, A.; Shinkai, M.; Honda, H.; Kobayashi, T. *J. Biosci. Bioeng.* **2005**, *100*, 1−11.

(4) Safarik, I.; Safarikova, M. *J. Chromatogr., B* **1999**, *722*, 33−53.

(5) Lund, V.; Schmid, R.; Rickwood, D.; Hornes, E. *Nucleic Acids Res.* **1988**, *16*, 10861−10880.

(6) Islam, D.; Lindberg, A. A. *J. Clin. Microbiol.* **1992**, *30*, 2801−2806.

(7) Inglis, D. W.; Riehn, R.; Sturm, J. C.; Austin, R. H. *J. Appl. Phys.* **2006**, *99*, No. 08K101.

(8) Furdui, V. I.; Harrison, D. J. *Lab Chip* **2004**, *4*, 614−618.

(9) Pamme, N.; Manz, A. *Anal. Chem.* **2004**, *76*, 7250−7256.

(10) Choi, J. W.; Oh, K. W.; Thomas, J. H.; Heineman, W. R.; Halsall, H. B.; Nevin, J. H.; Helmicki, A. J.; Henderson, H. T.; Ahn, C. H. *Lab Chip* **2002**, *2*, 27−30.

(11) Pamme, N. Magnetism and microfluidics. *Lab Chip* **2006**, *6*, 24−38.

(12) Gijs, M. A. M. Magnetic bead handling on-chip: new opportunities for analytical applications. *Microfluids Nanofluids* **2004**, *1*, 22−40.

* To whom correspondence should be addressed. E-mail: gwhitesides@gmwgroup.harvard.edu.

† Department of Chemistry and Chemical Biology.

‡ Department of Physics.

in biomedicine, and other areas, usually in systems that separate magnetic particles from diamagnetic media.[5,13-15] Magnetic media have been used, however, to separate diamagnetic particles, with ferrofluids providing the largest magnetic response.[16,17] Techniques for the levitation of diamagnetic particles in magnetic medium have developed as an alternative method to magnetic labeling techniques for separating diamagnetic materials.[15,18-21] In the past decade, the magnetic levitation of diamagnetic materials has become more accessible to standard laboratory facilities as the early experimental setup consisting of superconducting magnets (>10 T) and a pressurized oxygen atmosphere[22] has been replaced by small rare-earth magnets and aqueous paramagnetic salt solutions.[23-27]

As an extension of levitation, diamagnetic traps were developed to control, manipulate, and direct the positioning of cells and polymer microspheres suspended in solution.[28,29] In microfluidic systems, diamagnetic particles suspended in ferrofluid[30] or an aqueous paramagnetic solution[19,31] have been trapped and their trajectory manipulated while traversing the inhomogeneous magnetic fields. In this paper, we expand upon these label-free approaches and describe the design of a new device that exploits the principle of diamagnetic levitation to observe changes in density due to biological or electrostatic binding events and to separate and collect diamagnetic materials with different densities using a microfluidic system.

EXPERIMENTAL DESIGN

We designed and built a system for detecting and separating diamagnetic particles (5−5000 μm in diameter) based on differences in density. We will discuss two modes and uses of this system: a static mode—using no flow of fluid—as a diagnostic for detecting molecular or colloidal binding to polymer microspheres, and a flowing mode (within a microfluidic device) as a tool for continuously collecting separated diamagnetic particles. The system (in either mode) requires only simple components that include solutions of Gd^{3+} salts sandwiched between a set of rare earth magnets, like those shown in Figure 1, where z indicates the vertical direction.

(13) Haukanes, B. I.; Kvam, C. *Biotechnology* **1993**, *11*, 60−63.
(14) Oberteuffer, J. A. *IEEE Trans. Magn.* **1974**, *MA10*, 223−238.
(15) Simon, M. D.; Geim, A. K. *J. Appl. Phys.* **2000**, *87*, 6200−6204.
(16) Raj, K.; Moskowitz, R. *J. Magn. Magn. Mater.* **1990**, *85*, 233−245.
(17) Raj, K.; Moskowitz, B.; Tsuda, S. *Indian J. Eng. Mater. S.* **2004**, *11*, 241−252.
(18) Brandt, E. H. *Science* **1989**, *243*, 349−355.
(19) Watarai, H.; Namba, M. *J. Chromatogr., A* **2002**, *961*, 3−8.
(20) Franzreb, M.; Siemann-Herzberg, M.; Hobley, T. J.; Thomas, O. R. T. *Appl. Microbiol. Biotechnol.* **2006**, *70*, 505−516.
(21) Jayawant, B. V. *Rep. Prog. Phys.* **1981**, *44*, 411−477.
(22) Hirota, N. K. M.; Iwasaka, M.; Ikehata, M.; Uetake, H.; Takayama, T.; Nakamura, H.; Ikezoe, Y.; Ueno, S.; Kitazawa, K. *Physica B* **2004**, *346*, 267−271.
(23) Catherall, A. T.; Eaves, L.; King, P. J.; Booth, S. R. *Nature* **2003**, *422*, 579−579.
(24) Ikezoe, Y.; Hirota, N.; Nakagawa, J.; Kitazawa, K. *Nature* **1998**, *393*, 749−750.
(25) Ikezoe, Y.; Kaihatsu, T.; Sakae, S.; Uetake, H.; Hirota, N.; Kitazawa, K. *Energy Convers. Manage.* **2002**, *43*, 417−425.
(26) Kimura, T.; Mamada, S.; Yamato, M. *Chem. Lett.* **2000**, *11*, 1294−1295.
(27) Lyuksyutov, I. F.; Lyuksyutova, A.; Naugle, D. G.; Rathnayaka, K. D. D. *Mod. Phys. Lett. B* **2003**, *17*, 935−940.
(28) Kimura, T.; Sato, Y.; Kimura, F.; Iwasaka, M.; Ueno, S. *Langmuir* **2005**, *21*, 830−832.
(29) Winkleman, A.; Gudiksen, K. L.; Ryan, D.; Whitesides, G. M.; Greenfield, D.; Prentiss, M. *Appl. Phys. Lett.* **2004**, *85*, 2411−2413.
(30) Feinstein, E.; Prentiss, M. *J. Appl. Phys.* **2006**, *99*, No. 064901.
(31) Watarai, H.; Namba, M. *Anal. Sci.* **2001**, *17*, 1233−1236.

Figure 1. Schematic representations of the magnetic field, the distribution of magnetic forces, and a graph of the calculated magnitude of magnetic field along the axis of the magnets used for separation. (A) The calculated value of the magnitude of the magnetic field, $|\vec{B}|$, of the system is shown for a set of magnets, 50 mm long (L), separated by $(L/2)\sqrt{3} \approx 43$ mm. The shading in the plot indicates the magnitude of the magnetic field; the darker regions correspond to higher field intensities (white is ∼0 T and black is ∼0.4 T). This field was calculated using a finite element modeling software under axisymmetric boundary conditions. (B) Distribution of magnetic forces (eq 1) on diamagnetic material within our apparatus. The calculation shows that a diamagnetic particle would be repelled from the surfaces of the magnets and would be trapped along the axis between the magnets. (C) A graph of the calculated magnitude of the magnetic field in the vertical direction, B_z, along the axis between the two magnets (the dotted line in Figure 1A); the direction of a positive z-vector was chosen to be toward the upper magnet. The other components of the magnetic field along the chosen path are zero. Note that the gradient of the magnetic field in the vertical direction is constant—i.e., a constant slope in the variation of the magnetic field along the axis.

Theory for Density-Based Separations of Diamagnetic Particles. Density-based separations of diamagnetic particles are determined by the balance between the magnetic force and the buoyant force on a diamagnetic particle in a paramagnetic solution. In a static system, the force per unit volume ($\vec{F}/V$) on a particle in a magnetic field is the sum of the gravitational and magnetic forces (eq 1),[32]

$$\vec{F}/V = -(\rho_l - \rho_p)\vec{g} - \frac{(\chi_l - \chi_p)}{\mu_0}(\vec{B}\cdot\vec{\nabla})\vec{B} \qquad (1)$$

where the density of the liquid is ρ_l, the density of the particle is

(32) This equation is valid for systems in which $mB \ll kT$, the paramagnetic solution has no hysteresis, and the diamagnetic particle behaves as if it were in a continuous medium with a constant magnetic susceptibility. All three of these conditions are true in the system described here. Shevkoplyas, S. S.; Siegel, A. C.; Westervelt, R. M.; Prentiss, M. G.; Whitesides, G. M. *Lab Chip* **2007**, in press.

ρ_p, the acceleration due to gravity is $\vec{g}$, the magnetic susceptibilities of the liquid and the particle are χ_l and χ_p, respectively, the magnetic permeability of free space is μ_0, and the local magnetic field is $\vec{B} = (B_x, B_y, B_z)$. Both the magnetic field and its gradient contribute to the magnetic force and need to be optimized according to the dimensions of the system in order to maximize the separation. Equation 1 can be simplified for the levitation of a point particle—i.e., an infinitesimally small particle—in a system at equilibrium in which the magnetic field only has a vertical component (B_z); that is, the two other normal components of the applied magnetic field (B_x and B_y) are zero (eq 2).

$$(\rho_l - \rho_p)g = \frac{(\chi_l - \chi_p)}{\mu_0}B_z\frac{\partial B_z}{\partial z} \qquad (2)$$

The distribution of magnetic field is determined by the size, geometry, orientation, and nature or type of the magnets (Figure 1A). We used a set of solid-state NdFeB magnets (with length, width, and height of 5, 5, and 2.5 cm, respectively), having a magnetic field of ~0.4 T at their surface, to generate the required magnetic field and magnetic field gradient. Two magnets oriented toward each other in the design of an anti-Helmholtz coil established the magnetic field distribution in our system. In this geometry, the B_x and B_y components of the magnetic field are exactly zero only along the axis of the magnets, that is, along the vertical dashed line in Figure 1A, as confirmed by the completely vertical orientation of the force along this axis (Figure 1B). The B_z component of the magnetic field also becomes zero over this axis, but only at the midpoint between the two magnets. The effect of the magnetic force in this geometry is to attract the paramagnetic solution toward one or the other of the two magnets and, as a consequence, to trap all diamagnetic particles at the central region between the magnets (Figure 1B)—i.e., where $\vec{B}$ is close to zero. Equation 2 can be used to calculate approximately the balance of forces occurring on particles located along the axis of the magnets.

When the distance between the two magnets is $(L/2)\sqrt{3}$ times the radius of the magnets, the magnetic field profile is approximately linear and the gradient of the magnetic field is approximately constant in the z-direction (Figure 1C).[33] From eq 2, a constant gradient ($\partial B_z/\partial z$) yields an equal separation distance between pairs of particles of materials with similar differences in density ($\rho_l - \rho_p$); that is, for two diamagnetic particles, A and B, $z_A - z_B \propto \rho_A - \rho_B$. This configuration is the optimal arrangement for separating many particles that differ in density.

In order to separate diamagnetic objects with solid-state magnets, the solution must have a positive magnetic susceptibility. We used a paramagnetic aqueous solution of Gd^{3+}—as either $GdCl_3$ or the $Gd^{3+}\cdot DTPA$ complex. There are four characteristics of Gd^{3+} cations that are attractive for our system: (i) they (along with some of the other lanthanide cations) possess the largest magnetic susceptibilities ($\chi = +0.028 \text{ cm}^3/\text{mol GdCl}_3$) of any ionic species;[34] (ii) they permit straightforward visualization of samples because their solutions are colorless; (iii) they are compatible with proteins and cells when chelated (e.g., $Gd^{3+}\cdot DTPA$ complex);[29,35,36] and (iv) they have acceptable cost (salts of Gd^{3+} can cost <\$0.34/g salt = <\$0.80/g Gd^{3+} = <\$126/mol Gd^{3+}), and the solutions are reusable.

Since χ_p is negligible for all diamagnetic materials ($\chi_p \approx 0$), the magnetic force on a diamagnetic object is linearly proportional to the magnetic susceptibility of the paramagnetic solution (χ_l in eq 2). We use Gd^{3+} because it generates a larger magnetic force for a given concentration of cations and value of applied magnetic field than other transition metal cations. The exceptionally large magnetic susceptibility of Gd^{3+} (compared to the susceptibilities of other lanthanide cations), enables the system (i) to levitate particles with greater density for an equal concentration of paramagnetic cations and (ii) to levitate a given particle using a lower concentration of paramagnetic ions.

RESULTS AND DISCUSSION

Scope of Density-Based Detections and Separations. We performed several experiments to explore the useful range of densities appropriate for our system.

Densities of Particles for Separations in Aqueous Solutions. We determined the separation range and resolution of a system having the magnetic field distribution illustrated in Figure 1B using aqueous solutions containing concentrations of Gd^{3+} from 0.4 to 1.9 M. We placed a bead of known density (from a set of ~6-mm glass beads with densities ranging from 1.1500 to 1.8000 g/cm³ (± 0.0001 g/cm³)) into a vial filled with an aqueous $GdCl_3$ solution, aligned the vial with the axis of the magnets, and recorded the height (h in Figure 2B) to which the center of the bead levitated (Figure 2). From these experiments, we determined that particles with densities up to 1.8 g/cm³ could be levitated with our system at different concentrations of Gd^{3+}. This limit was established by maximizing both ρ_l and χ_l (eq 2), which maximizes the magnetic force and the buoyancy of the solution. Particles more dense than the Gd^{3+} solution (i.e., $\rho_p > \rho_l$) would levitate at positions below the midway point between the two magnets. By contrast, particles having a density lower than the Gd^{3+} solution (i.e., $\rho_p < \rho_l$) would levitate in the upper half of the space between the magnets and determine the lowest densities that can be levitated in the system.

The difference between the densities of two diamagnetic particles, A and B, is proportional to the magnetic susceptibility of the Gd^{3+} solution (χ_l) and to the difference between their levitation heights: $\rho_A - \rho_B \propto (\chi_l (z_A - z_B))$. As a result, for a given difference in density between two diamagnetic particles, the distance between their levitation heights will decrease as the magnetic susceptibility of the solution increases (i.e., as the concentration of gadolinium increases, Figure 2A). The concentration of Gd^{3+} in solution should, therefore, be chosen to balance two requirements. The magnetic susceptibility of the solution must be (i) sufficient to levitate the particles but (ii) as low as possible to maximize the sensitivity of the system—that is, to maximize the ability of the technique to separate materials with similar densities.

We could separate beads with differences in density of 0.05 g/cm³ (Figure 2A). The sensitivity of the system could be

(33) Purcell, E. M. *Electricity and magnetism*; McGraw-Hill, Inc.: New York, 1985.
(34) Berger, L. I., Ed. *CRC Handbook of Chemistry and Physics*, 85th ed.; CRC Press LLC: Boca Raton, FL, 2000.

(35) H. Gries, D. R.; Weinmann, H.-J. Sterile pharmaceutical compositions of gadolinium chelates useful NMR imaging. U.S. Patent 4,957,939, September 18, 1990.
(36) U.S. Food and Drug Administration. Information on gadolinium-containing contrast agents. http://www.fda.gov/cder/drug/infopage/gcca/default.htm (accessed Mar 2007).
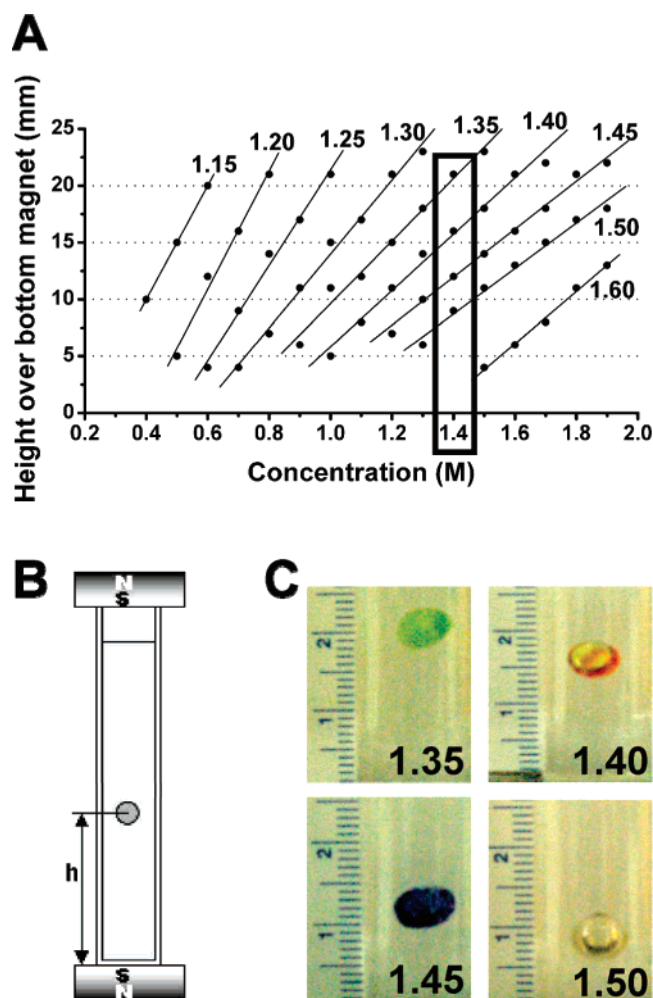
Figure 2. Calibration of the effective density gradient for aqueous solutions containing different concentrations of $GdCl_3$. The calibration was performed using a set of 5−8-mm glass spheres with densities specified to 0.0001 g/cm³. (A) A graph illustrating the range of densities that can be levitated for concentrations of $GdCl_3$ from 0.4 to 1.9 M. The separation between any two successive data points for any given concentration is approximately equal. The numerical label for each line corresponds to the density of the sphere (in g/cm³). (B) A schematic showing the experimental design from which we obtained the data. The "h" in the figure corresponds to the height in the graph to which a sphere of known density levitated. (C) Photographs of the levitated spheres for the 1.4 M $GdCl_3$ solution that is highlighted in (A). The number on each picture corresponds to the density of the glass sphere.

optimized by (i) working at the concentration of gadolinium that maximizes the difference in levitation height and (ii) using a high-resolution optical recording device (camera). The use of digital image processing techniques could help to discriminate closely positioned materials and thus further increase the sensitivity of the system.

Densities of Particles for Separations in Nonaqueous Solutions. Nonaqueous solutions have densities different from those of aqueous solutions and can be used to expand the range of densities of materials that this system is able to separate. We used, for example, a methanol solution containing $GdCl_3$ to levitate various polymers with densities between 0.90 and 1.05 g/cm³: isotactic polypropylene (PP), polyethylene (PE), and polystyrene (PS). We chose methanol for our solvent because (i) it has a density of 0.792 g/cm³, a value lower than that of both water and
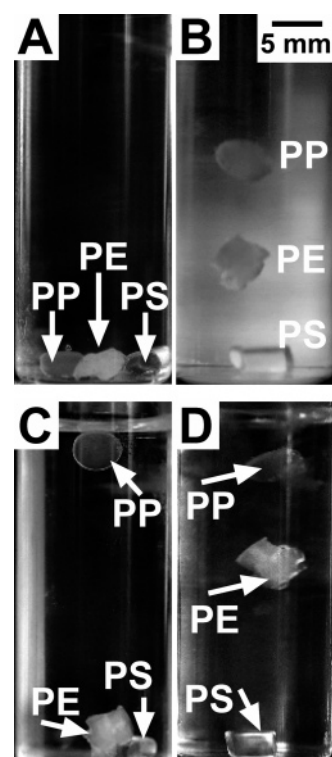
Figure 3. Photographs of a methanol solution containing $GdCl_3$ and pieces of PP, PE, and PS outside and inside the magnetic field configuration. (A) A 360 mM $GdCl_3$ solution in methanol in the absence of the magnetic field. Since this solution was less dense than the polymers, the polymers sank to the floor of the vial. (B) In the applied magnetic field, the PP and PE particles levitated while the PS particle remained on the floor of the vial. (C) A 435 mM $GdCl_3$ solution in methanol in the absence of a magnetic field. PP was less dense than the solution and it floated at the air/methanol interface. (D) The 435 mM $GdCl_3$ solution containing the same polymer pieces (as in (C)) in an applied magnetic field. The PP particle submerged in the solution under the influence of the magnetic force acting parallel to the gravitational force.

most polymers, (ii) it is a good solvent for dissolving inorganic salts (we could prepare a solution of 1 M $GdCl_3$ in methanol), (iii) it does not swell PDMS,[37] and (iv) it does not dissolve most hydrophobic polymers, including PP, PE, and PS.

Many common industrial plastics have densities less than that of water—for example, the densities of PP and PE are 0.90 and 0.93 g/cm³, respectively. When we placed a piece of PP, PE, and PS (which is more dense than water, $\rho = 1.05$ g/cm³) in a vial containing a 360 mM $GdCl_3$ solution of methanol, all three polymers sank to the bottom of the vial in the absence of an applied magnetic field (Figure 3A). After aligning the vial with the axis of the magnets, both PP and PE pieces levitated to different heights; the PS did not levitate and remained on the bottom of the vial (Figure 3B).

An interesting physical phenomenon occurred when we placed a piece of PP, PE, and PS in a 435 mM $GdCl_3$ solution in methanol. In the absence of a magnetic field, PS and PE sank to the bottom of the vial, but PP—the least dense polymer—floated at the air/methanol interface (Figure 3C). When the vial was aligned with the axis of the magnets, PE levitated and the more dense PS remained on the bottom of the vial as expected, but surprisingly,

(37) Lee, J. N.; Park, C.; Whitesides, G. M. *Anal. Chem.* **2003**, *75*, 6544−6554.

the magnetic force pulled the PP into the solution (Figure 3D). As reported previously,[38] this apparent enhancement of the gravitational force is due to the negative sign of the z-component of the magnetic field above the midway point between the two magnets. Equation 2 and Figure 1C show that, if the particle is located above that height, the magnetic force is negative and acts in the same direction as the gravitational force.

Density-Based Detection. *Detection of Protein Binding to a Solid-Supported Small Molecule.* We used density differences as a label-free method for detecting biological binding events. We demonstrated this principle by observing the differences in height of levitation of biotin-labeled PEGA polymer (an acryloylated *O,O′*-bis(2-aminopropyl)poly(ethylene glycol)/dimethylacrylamide copolymer) in the presence and absence of streptavidin, a 53-kDa protein. Beads of biotin-labeled PEGA polymer swell in water (unlike polystyrene-based solid supports), have a loading capacity of 0.2 mmol of amine/g of PEGA and pores of sufficient size for ~70-kDa proteins to access the biotin on the interior of the polymer.[39] The sensitivity of detection depends directly on the loading capacity (i.e., surface density of reacting groups) of the beads and the molecular weight of the bound molecules. In initial experiments, we observed precipitation after adding proteins to the aqueous Gd^{3+} solution; so instead, we used the $Gd^{3+}·DTPA$ chelate to circumvent this problem.

We detected binding of streptavidin to solid-supported biotin by incubating ~20 water-saturated polymer beads with 20 μL of 0.19 mM protein dissolved in 40 mM potassium phosphate buffer (pH 7.0). After 15 min, we diluted the solution to 1.5 mL to suspend the beads using 210 mM $Gd^{3+}·DTPA$ in 40 mM potassium phosphate buffer (pH 7.5) and then added ~20 more biotin-labeled polymer beads. We mixed the solution gently for 5 s with a spatula and then inserted the cuvette along the axis of the magnets. After ~30 min, all of the beads had clustered into two separate bands (Figure 4A), the upper one levitating at the same height as the unlabeled PEGA polymer. The lower, denser band reflected the binding of streptavidin to the solid-supported biotin.

The specific recognition of streptavidin was confirmed using two control experiments: (i) the binding experiment was repeated with unlabeled PEGA polymer (Figure 4B). In this experiment, we observed only the top band, with no obvious nonspecific adsorption of streptavidin to the polymer beads; and (ii) the binding experiment was repeated using a 1:1 solution of 0.2 mM fluorescein-labeled streptavidin (FITC-streptavidin) and 0.2 mM unlabeled streptavidin dissolved in 40 mM potassium phosphate buffer (Figure S-1 Supporting Information). In this case, the beads that were exposed to streptavidin were fluorescent, while the unexposed beads were white.

Electrostatic Adhesion of Gold Nanoparticles to Chemically Modified Microspheres. Gold nanoparticles bound to polymer spheres alter the effective density of the spheres. We used magnetic levitation to observe this change in density of the spheres. Cross-linked polystyrene microspheres (~50 μm in diameter) were chemically modified to yield microspheres with tetraalkylammonium chloride functionality ($PS-CH_2NR_3^+$ Cl^-; NR_3 = quinuclidine); these spheres are positively charged.[40] We combined these spheres in a 1:1 water/DMF solution with gold
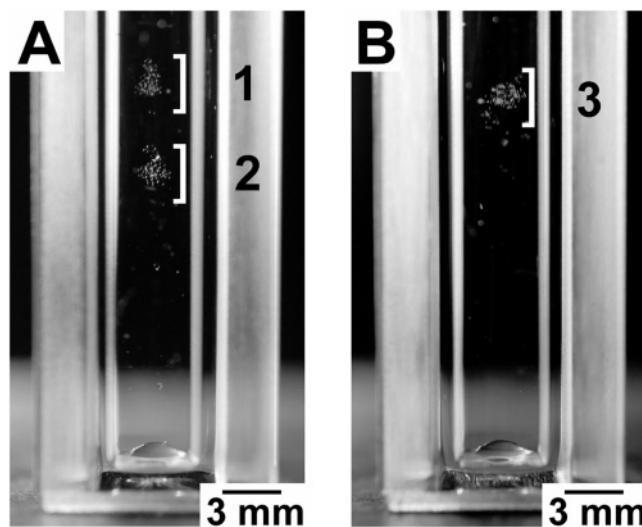
Figure 4. Optical images of the separation and control experiments demonstrating the detection of streptavidin. (A) Separation of biotin-labeled PEGA polymer that was exposed to a solution of streptavidin (2) from a set of biotin-labeled PEGA polymer that was not exposed to streptavidin (1). (B) Unlabeled PEGA polymer that was exposed to streptavidin mixed with unlabeled PEGA polymer that was not exposed to streptavidin (3). Both types of polymer beads levitate at the same height.

nanoparticles (~12-nm diameter) capped with a citrate layer; these gold nanoparticles are negatively charged. The nanoparticles condensed onto the surface of the microspheres due to electrostatic attraction; after 1 h, we filtered and collected the microspheres. In an aqueous, 300 mM solution of $GdCl_3$, we mixed the Au-bound spheres with similar tetraalkylammonium-functionalized microspheres that were not bound to Au and aligned the vial containing this solution with the axis of the magnets. After the beads reached their equilibrium position (~20 min), two distinct bands of beads formed in the system (Figure 5). The Au−spheres appear purple due to the aggregation of gold nanoparticles. The separation between the two bands is small because the increase in density to a polymer sphere by the attachment of a thin layer of gold nanoparticles is ~0.02 g/cm^3. The variation observed in the separation could be due to the amount of gold bound to each sphere, the degree that each sphere was functionalized, or differences occurring in the fabrication of the beads. These results demonstrate that the magnetic levitation device can detect the change in density that accompanies binding of heavy-metal colloids to polymer beads.

Density-Based Separation. We extended the magnetic levitation of label-free diamagnetic particles from a static mode to a microfluidic system that enables separation and collection of the particles with different densities.

Design of the Microfluidic System. We built the system as a microfluidic device to take advantage of laminar flow: that is, flow in streams without turbulence that would disrupt separations.[41] Microfluidic systems also use only small volumes of sample and solution. The microfluidic device consisted of a PDMS replica, fabricated using soft lithography,[42,43] and sealed to a glass slide.[44] PDMS and the glass slide are transparent and enable straightforward visualization of the separation.

(38) Yamato, M.; Kimura, N. H. *Langmuir* **2002**, *18*, 9609−9610.

(39) Meldal, M.; Svendsen, I. *J. Chem. Soc., Perkin Trans. 1* **1995**, *12*, 1591−1596.

(40) McCarty, L. S.; Winkleman, A.; Whitesides, G. M. *Angew. Chem., Int. Ed.* **2006**, *46*, 206−209.

(41) Squires, T. M.; Quake, S. R. *Rev. Mod. Phys.* **2005**, *77*, 977−1026.

(42) Xia, Y. N.; Whitesides, G. M. *Annu. Rev. Mater. Sci.* **1998**, *28*, 153−184.

(43) Gates, B. D.; Xu, Q. B.; Stewart, M.; Ryan, D.; Willson, C. G.; Whitesides, G. M. *Chem. Rev.* **2005**, *105*, 1171−1196.
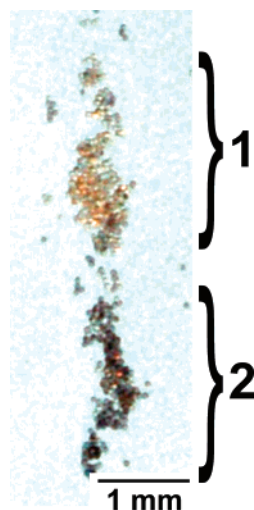
Figure 5. Photograph of the separation between microspheres modified with tetraalkylammonium chloride functionality having gold nanoparticles electrostatically attached to the surface (2) and similarly modified microspheres without adsorbed gold (1). The beads with adsorbed gold colloidal particles are denser than those without gold, and therefore, they settle lower in the system. The spread in height within each set of beads likely is due to variations in the sizes of the beads (they are polydisperse), which results in varying densities.

For ease of description, we divide the fluidic system into four sections (shown in Figure 6): the injection system, the separation device, the collection system, and the exhaust.

(I) Injection System. A syringe pump injected the sample from a syringe held vertically (i.e., normal to the laboratory bench) at a height (*H*) above the separation device. This orientation allowed the combination of the fluidic forces and the gravitational forces to direct the beads into the separation device (eq 2). Other orientations of the syringe pump were less successful: when the syringe was held horizontally, for example, the microspheres settled inside the barrel and did not flow into the tubing. In principle, we could remove the syringe pump and use gravity-driven flow exclusively; this change would enable the system to run without electricity.

(II) Separation Device. The triangular PDMS channel was placed vertically (*z*-direction) between the magnets, with its wide edge aligned with the axis of the magnets. The shape of the channel minimized regions with low or zero flow rate (i.e., dead volume) so that all particles would flow from a single inlet to multiple outlets across the separation device. In the absence of flow, the diamagnetic particles would levitate along this axis, as discussed previously. The laminar flow through the channel has both *y*- and *z*-components because of the triangular shape of the channel; this additional *z*-component to the total force creates a slight difference in the observed height between the static mode and flowing mode. We were able to separate 75−150-μm spheres over a range of flow rates from 0.10 to 0.25 mL/min. For sample volumes ranging from ~100 μL to several milliliters, these flow rates yielded separation times from minutes to over 1 h, respec-

tively. We chose the flow rates so that the time required for the beads to flow across the separation device was longer than that required for the system to reach equilibrium in the magnetic field; in this laminar, quasi-equilibrium protocol, the beads separate in the applied magnetic field before they reach the outlet of the microfluidic device.

(III) Collection System. After passing through the separation device, the only forces acting on the particles are fluidic forces and gravity. We designed the collection system to simplify the removal of samples from the device. Every outlet from the PDMS separation device leads to a separate glass vial with a septum top to maintain a sealed fluidic system. These vials were positioned lower than the device to facilitate gravitational settling of the beads, to enhance the rate of collection into the glass vials, and to minimize clogging of the tubing. Easy removal of the septum tops from the vials permitted simple collection of each sample after the experiment was complete without disrupting the tubing or the fluidic connections.

(IV) Exhaust System. We designed the exhaust system to maintain a constant flow rate throughout the entire setup. Each collection vial was attached to an exhaust tube that remained open to the atmosphere. The exhaust tubes were held above the device at the same height (*H*) as the syringe for injection. This configuration provided a constant back pressure to the system and prevented a pressure drop due to gravity between the outlet at the bottom of the device (nearest the lower magnet) and the outlet at the top of the device. This exhaust system ensured that all the outlets experienced the same flow rate.

Optimization of Parameters for the Flowing System by Means of Static-Mode Tests. Before employing the microfluidic system, we carried out static experiments to characterize the steps needed for sample preparation and to determine experimentally the concentration of GdCl$_3$ for optimal separation between particles.

Merrifield resins, formed by copolymerization of styrene, divinylbenzene, and vinylbenzyl chloride, are common substrates for solid-phase synthesis; the ones we used were beads with diameters in the range of 75−150 μm. Different batches of Merrifield resins contain different relative amounts of backbone-attached CH$_2$Cl groups; these differences are reflected in different chlorine content for each batch (0.38, 1.06, 1.24, or 1.95 mmol of Cl/g of polymer, for the samples examined here). These differences in chloromethyl functionality result in different mass densities for each batch.

In a solution containing 250 mM GdCl$_3$, we separated all four batches of beads. Merrifield resins taken directly from the vendor were nonuniform in density and yielded broad distributions that complicated the collection of single batches of particles (Figure 7A). In the magnetic field, the least dense batch of beads (0.38 mmol of Cl/g of polymer) floated on the solution/air interface and would not traverse the microfluidic system.

To circumvent this problem, we swelled the beads in toluene, rinsed the spheres in ethanol and then in water, and dried them in a 120 °C oven. After this procedure, the density of the spheres became more uniform and slightly greater for all batches (Figure 7B). We suspect that the swelling and deswelling process (soaking in toluene followed by rinsing with water) removed any air trapped within the sphere during manufacturing and allowed the polymer to reorganize into a more densely packed structure.

(44) Ng, J. M. K.; Gitlin, I.; Stroock, A. D.; Whitesides, G. M. *Electrophoresis* **2002**, *23*, 3461−3473.
(45) Shipway, A. N.; Lahav, M.; Gabai, R.; Willner, I. *Langmuir* **2000**, *16*, 8789−8795.
(46) Weibel, D. B.; Lee, A.; Mayer, M.; Brady, S. F.; Bruzewicz, D.; Yang, J.; DiLuzio, W. R.; Clardy, J.; Whitesides, G. M. *Langmuir* **2005**, *21*, 6436−6442.
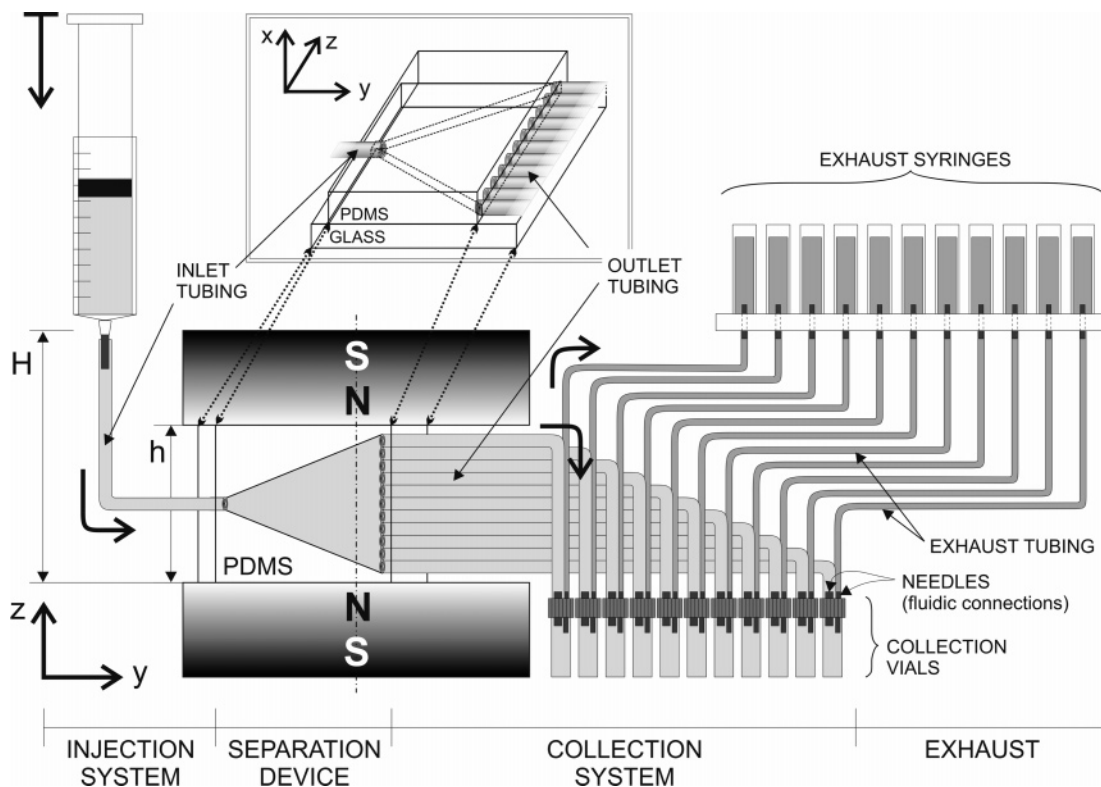
Figure 6. Schematic representation of the separation and collection system illustrating the four sections of the system: (i) injection system, (ii) separation device, (iii) collection system, and (iv) exhaust. A PDMS channel is placed between two permanent rare earth magnets with the direction of the fluid flow orthogonal (y) to the direction of the poles of the magnets (z). A triangular geometry for the channel was used to minimize the volume within the channel that experienced a minimal or zero flow rate. The inset highlights the PDMS chamber sealed to a glass slide and shows both the inlet and the outlet tubing.

We dyed each type of Merrifield resin with a different dye to allow clear visualization of the separation: 0.38 mmol of Cl/g of polymer dyed blue; 1.06 mmol of Cl/g of polymer dyed red; 1.24 mmol of Cl/g of polymer dyed orange; 1.95 mmol of Cl/g of polymer dyed green. The distribution of bands of the dyed polymers created in the presence of the magnetic field appeared similar to that observed for the same batches of nondyed spheres (Figure 7B compared to Figure 7C).

To confirm that this dyeing process did not alter the densities of the spheres, we dyed two sets of beads with identical densities (0.38 mmol of Cl/g of polymer) with two different dyes—blue and yellow—and left a third set of beads with the same density undyed. All three sets of spheres levitated at the same height in the channel (Figure 7D). The three sets of spheres appeared randomly dispersed throughout the cluster of beads; this observation establishes that no separation occurred and that any deviation in density due to the dyeing process was negligible. In static tests, we achieved optimal separation with an aqueous 250 mM GdCl$_3$ solution containing beads that were prewashed, dried, and dyed with various organic dyes.

Dynamic, Flowing Separation and Collection. Having optimized the static separation of four different batches of Merrifield resins, we transferred the conditions to the system using flowing liquids. We filled the system with an aqueous 250 mM GdCl$_3$ solution and introduced the mixture of dyed spheres with a syringe pump. The spheres entered the separation channel from a single inlet on the left (Figure 8A) and exited through multiple collection outlets on the right (Figure 8B).

The results of the separation are reported graphically in Figure 8C. The device is capable of separating all four of the different batches of beads, even when the batches are present in unequal proportions—in Figure 8, more blue beads are present than any of the other types. The reason that the green spheres, the densest spheres, have the least number of collected particles is because they traversed the separation device along the bottom of the PDMS channel, where some of the beads stuck to the bottom wall of the channel and others were caught at the junction of the outlet tubing and the PDMS microfluidic device.

The separation of particles in a flowing system is a nonequilibrium process: the particles are affected by fluidic, gravitational, and magnetic forces. A particle entering the separation device experiences both fluidic and magnetic forces in the positive y-direction. After a particle passes the axis of the magnets (dotted line in Figures 2 and 8A), the B_y component of the magnetic field becomes negative, and thus, the magnetic force ($-y$-direction) opposes the fluidic drag force ($+y$-direction). We observed some clustering of the particles over the axis of the magnets due to the change in sign of the y-component of the magnetic force (Figure 8A).
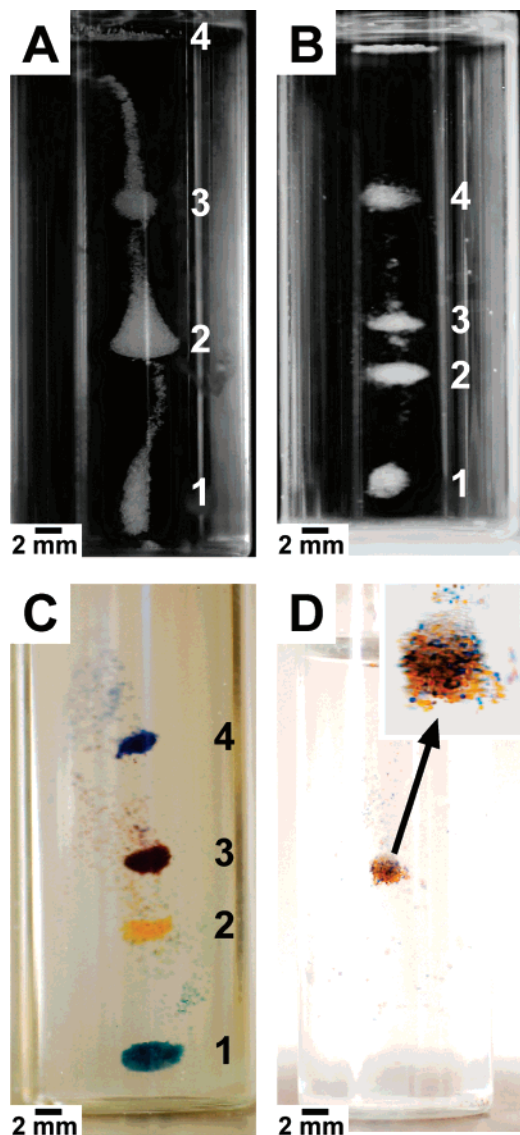
Figure 7. Photographs of the static system and the four batches of Merrifield resins with different degrees of functionality (from the bottom to the top of the channel is (1) 1.95, (2) 1.24, (3) 1.06, and (4) 0.38 mmol of Cl/g of polymer). (A) Separation of the spheres as received from the manufacturer. (B) Separation of the beads after washing and drying them. The densities of the spheres increased and became more uniform. (C) Separation of the beads after dyeing them with organic dyes. (D) Levitation of three sets of a single batch— 0.38 mmol of Cl/g of polymer. Beads of the same batch, but dyed blue or orange, levitate to a similar height as undyed beads.

CONCLUSION

This paper demonstrates the ability to levitate, and to separate, diamagnetic particles suspended in solutions containing paramagnetic cations using an inhomogeneous magnetic field. We describe a microfluidic device based on diamagnetic levitation that is able to separate and collect continuously polymer particles that differ in density. We also present a new method for detecting specific protein and nanoparticle binding to polymer beads.

The major advantages of this separation device are the following: (i) it is a simple apparatus that does not require electric power (only a set of permanent magnets is required); (ii) it is transparent (neither PDMS nor solutions containing Gd^{3+} cations absorb visible light); (iii) it is simple to collect the separated
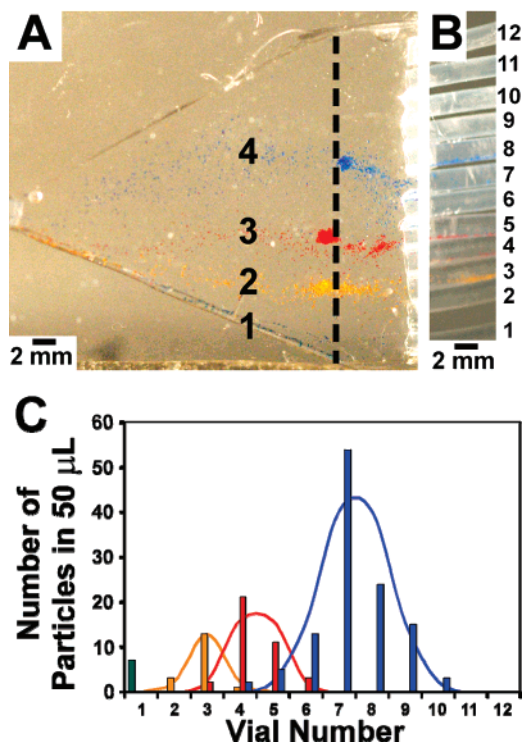
Figure 8. Photographs of four different Merrifield resins with different amounts of chloromethyl functionality separated in the magnetic apparatus shown in Figure 6. The degree of functionality of the spheres from the bottom to the top of the channel is (1) 1.95, (2) 1.24, (3) 1.06, and (4) 0.38 mmol of Cl/g of polymer. (A) An image of a flowing separation in a microfluidic device. The flow goes from left to right and the beads are separated by the magnetic field and collected in the 12 outlet channels on the right. The dotted line is the location of the axis of the magnets. (B) An image of the outlet tubing several centimeters downstream near the conclusion of the experiment illustrating successful separation and collection of the particles. (C) A histogram of a sample population of beads collected from the vial attached to each outlet tube as labeled in (B). This graph illustrates the successful separation and collection of spheres that differ in density.

particles for further processing; and (iv) it does not require initial functionalization of the particles to magnetic supports. The limitations of this system are as follows: (i) it requires ionic species in high concentrations (>100 mM), and (ii) it is unable, in its current form, to separate very small particles (<1 μm).

Density separation is an important and ubiquitous technique, often accomplished by centrifugation. We expect the technique described here to be useful for purifying large quantities of samples since continuous flow and separation are possible. Several devices also may be linked in parallel to improve resolution with minimal extra cost. We hope that the type of separation presented here will be useful in remote settings and in resource-poor regions: the system requires no electricity, the apparatus and paramagnetic solutions are reusable, and the readout is accomplished by eye.

SUPPORTING INFORMATION AVAILABLE

Additional information as noted in text. This material is available free of charge via the Internet at http://pubs.acs.org.